International Research Journal of Engineering and Technology (IRJET) e-ISSN: 2395-0056
Volume: 07 Issue: 11 | Nov 2020 www.irjet.net p-ISSN: 2395-0072

A Simplified Approach for Analysing Non-uniform Structure in Integrated Optics

Belghoraf Abdelrahmane

Electronics Eng. Department, University of Sciences and Technology of Oran, BP 1505 Mnaouer, 31000, Oran, Algeria.

Abstract: This paper analyzes a non-uniform structure known as a tapered waveguide in integrated optics applications using locally the conventional electromagnetic wave theory. Hereby, the tapered structure is visualised as a series of uniform steps, in which conventional wave theory for uniform guides holds. The solution of Helmoltz equation is accomplished by suggesting in each medium, as well as in each region, appropriate solutions of the field which satify the local boundary conditions.

Keywords

Integrated Optics, Thin Film Waveguide, Fiber Optics.

1. Introduction

This article analyzes the plane parallel waveguide using the conventional electromagnetic wave theory which provides a framework for comparison with other references. We consider the structure and co-ordinate system shown in Fig. 1, where a film of range dependent thickness T and a uniform index n_1 is shown. As light propagating in the structure of Fig.1, it is confined by total internal reflection. In order to achieve true mode guidance, it is necessary to require that

$n_1 > n_2 > n_3$. (1)

For numerical purposes, we shall mostly fix the indices as follows:

$n_1 = 2$; $n_2 = 1.76$; $n_3 = 1$. (2)

These values are not intended to be exactly typical in integrated optics devices, but have been chosen arbitrary.

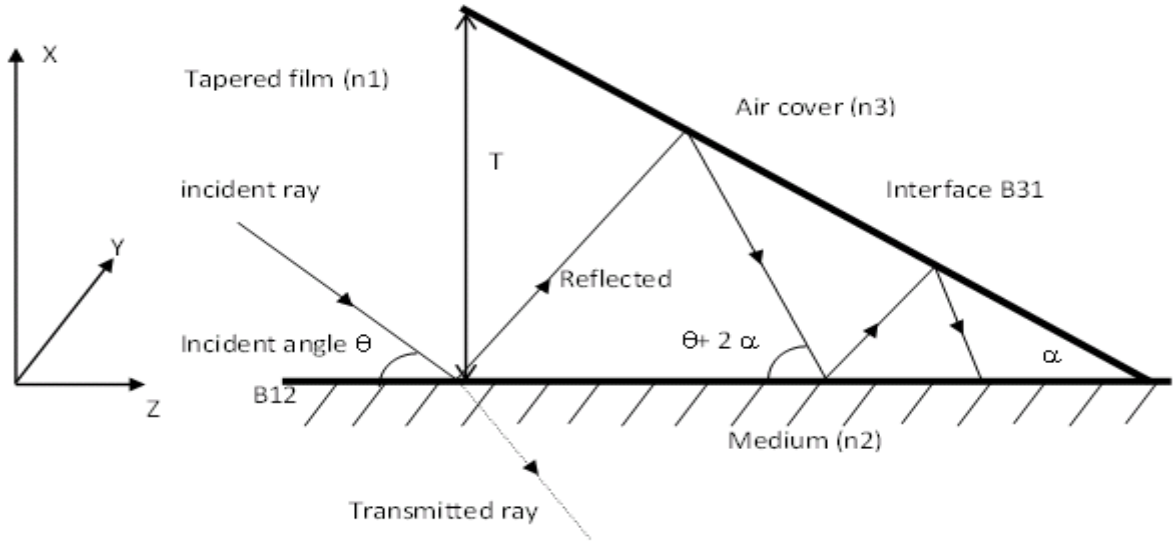

Fig. 1 : Configuration of the non-uniform structure to be analyzed (tapered waveguide).

We shall assume throughout this article that the waveguides of Fig. 1 consist of media which are lossless and isotropic. For a discussion of lossy and anistropic media, the reader should refer to refs. [1-3] .

The physical picture of light guidance is one of the light rays tracing a multiple-reflected path in the tapered film (n_1), (see Fig. 1).

We establish the convention that the B_{ij} boundaries refer to the interface between media of refractive index n_i and n_j. As such zigzag rays propagate into the tapered film (n_1), and each successive pair of reflections at the boundaries B_{12} and B_{31} increase the angle of incidence θ by twice the wedge angle α . Eventually, this angle θ will be higher than the critical angle θ_c (defined as $\theta_c = A\cos n_2 / n_1$), for total reflection at B_{12} then, some energy begins to leak into the medium (n_2). Note that the critical angle at B_{31} is higher than the critical angle at B_{12}, as one has appropriately chosen the indices in Eq. (2). Hence, radiation leaks (coupling) occur at the B_{12} boundary before they occur at B_{31} boundary.

The tapered waveguide (n_1) constitutes the main body of the structure of Fig. 1 to be analysed. In order to enable the derivation of mode characteristics and to analyze this structure, that is to say to elaborate and predicates the field distribution behaviour along the guiding structure; we could approximate the tapered film (n_1) by sequence of steps that discretely represent the taper of Fig. 1. Obviously, the result improves as the steps are made smaller in size and greater in number (see Fig. 2). Within each step the solutions for the modes are simply those of a waveguide with parallel boundaries. Each step will be characterized by its thickness T.

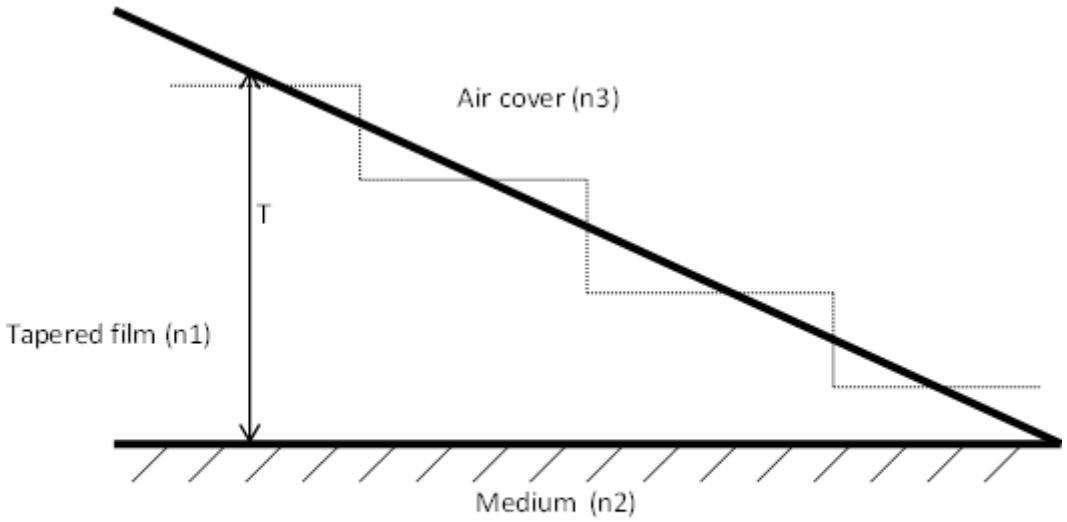

Fig. 2 : Approximation of the tapered waveguide (n1) by using a series of steps

The problem of calculating the amplitude characteristic of the transmitted and reflected modes at each step , for a given incident ray , is done by matching the incident , reflected and transmitted field components at each step boundary [4] . We shall therefore analyze the structures locally as though they were translation-invariant in configuration. Such planar structure is illustrated in Fig. 3 corresponding to the structure of Fig. 1. Thereby we define the co-ordinate systems. We use the conventional electromagnetic wave formalism to introduce the basic concept and terminology of the structure of Fig. 3, including the nature of mode propagation, waveguide cut-off and propagation constants. We assume invariance of the physical geometries along the y-axis which symbolically expresses the fact that all derivatives with respect to the y-axis are zero. When a wave propagates inside the structure, one dimension of the beam cross-section is guided by the stratification of the layers in x; but in the z-direction, the wave can propagate freely. Also fields of the guided modes must vanish at $|x| = \infty$. An appropriate field pattern is required inside and outside the film (n_1) so that the desired coupling to adjacent layers can be achieved.

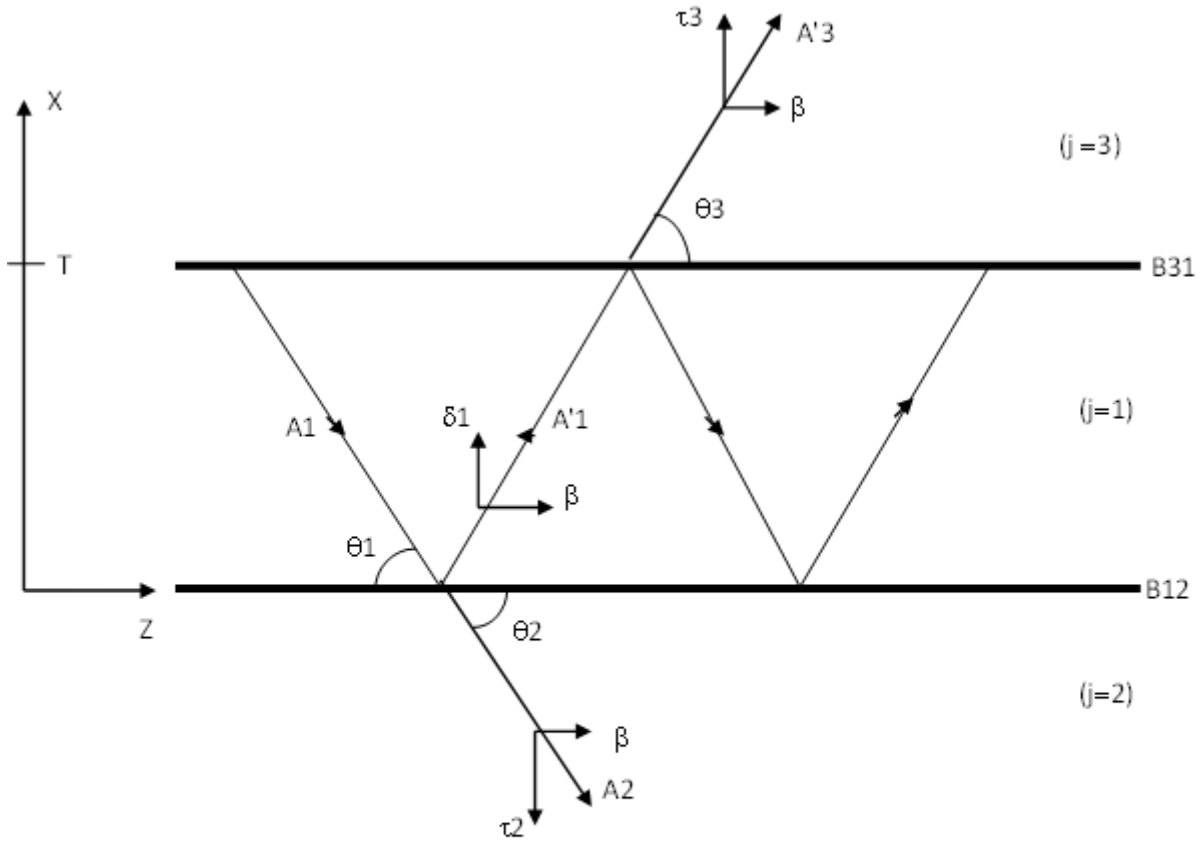

Fig. 3 : Wave tracking in each medium (j) of each step of

Fig. 2 at a local thickness T ; the tapered film (n1) of

The modal field for a plane parallel structure can be derived from the one-dimensional modal equation (for TE modes) [3].

$$\frac{d^2 E_y}{dx^2} + (\text{nj } k_0 - \beta)\, Ey = 0, \quad (3)$$

where :

$$\beta = k_0\, n_j \cos(\theta_j), \quad (4)$$

k_0 is the free-space wave number. The subscripts θ_j and n_j respectively relate to the angle of modal plane wave and the index of the layer concerned. Equation (4) defines the so-called modal propagation constant.

Mathematically, problems involving Maxwell's equation have solutions that match the boundary conditions at interfaces. Various modes of propagation can be discerned in these geometric configuration of Fig. 3. Thereby, modal fields are either trapped in the film layer (n_1) or are radiation modes in the surrounding materials; medium (n_2) or medium (n_3). In each of the layers of Fig. 3, we shall postulate plane-wave electric fields E_y. As the TE mode has only three field components H_x and H_z can be derived straight away from E_y by means of Maxwell's equations [5]. The customary time dependence in complex notation can be expressed by exp(-i ω t), and will be omitted throughout the equations still to come. We shall use the subscript j =3 for the quantities that belong to free-space 2 and 1 ; for the quantities that belong respectively to the films (n_2) and (n_1), see Fig. 3. We shall denote the complex amplitude of the downward and upward plane waves by A_j and A'_j in each medium. Conventionally, all A_j waves propagate towards the lower boundary, and the A'_j towards the upper

boundary, see Fig. 3. When coupling of waves in each medium occurs, all waves have the same propagation constant β , defined in Eq. (4).

2. Analysis of Cross Section of Field Pattern

We shall consider two cases as waves propagate along the parallel films of Fig. 3.

a) Guided Wave Region

In this region, plane waves in the film (j = 1) impinge at an incident angle θ_1 to the boundaries which renders the effective index (defined as β/k_0) in the interval $n_2 < \beta/k_0 < n_1$.In others words, $\theta_1 < \theta_c$. The guided wave modes are the transverse elctromagnetic waves trapped inside the film (j=1) by total internal reflection between B_{12} and B_{31} boundaries.

Because of the total internal reflection in the film (j =1), the electromagnetic field is non zero in the lower-index regions but, the amplitude of the wave decays exponentially as a function of the cross distance x in those regions.

We define the transverse propagation constants as:

$\delta^2_j = n^2_j\, k_0 - \beta^2$ j = 1, (5)

$\tau_j = \beta - n_j\, k_0$ j = 2,3 , (6)

$\beta = k_0\, n_j \cos(\theta_j)$ j = 1,2,3, (7)

where β is the longitudinal propagation constant , δ_j is the real transverse propagation constant in a medium where oscillating waves are present and τ_j is the evanescent transverse decay constant corresponding to a medium where evanescent waves are present .

The distribution of the electromagnetic field component has the form of a standing wave in the film (j=1), and exponential in mediums (j=2) and (j=3). That is to say:

$E_y = A_j\, \mathrm{Exp}(- x\, |\tau_j|)$ j = 3, (8a)

$E_y = A_j\, \mathrm{Exp}(- j\, x\, \delta_j) + A_j'\, \mathrm{Exp}(j\, x\, \delta_j)$ j = 1 , (8b)

and

$E_y = A_j\, \mathrm{Exp}(x\, |\tau_j|)$ j= 2 . (8c)

We also define the derivatives of the electromagnetic field components as :

$$i\,\omega\,\mu\, H_x = -\frac{dE_y}{dz} \quad , (9a)$$

and

$$i\,\omega\,\mu\, H_z = \frac{dE_y}{dx} \quad , (9b)$$

where ω and μ are the pulsation of the wave and the permeability of the concerned solid media , respectively .

The boundary conditions demand that the field E_y and its normal derivatives be continuos across the boundaries :

x = 0 and x = T , (10) where T represents the physical local thickness of the film (j=1) .

Normalizing the modes to a unit power P, requires :

$$P = \frac{1}{2}\ \text{Real}\left[\int_{-\infty}^{+\infty} E_y \times H_x^{*}\, dx\right] = 1\ , (11)$$

where P represents the total transverse power across the structure , and the asterisk denotes the complex conjugate of the H_x component defined in Eq. (9) . Application of Eqs. (8) through (11) leads to the determination of the field amplitudes A_j and A'_j . and to the characteristic equation : $T\,\delta_1 - \text{Atan}\left(\frac{|\tau_3|}{\delta_1}\right) - \text{Atan}\left(\frac{|\tau_2|}{\delta_1}\right) = q\,\pi$, (12)

where the integer q is the mode number , and the transverse propagation constants are given by Eqs. (5) and (6) . Equation (12) is the characteristic equation for the structure of Fig. 2 in the pure guided wave region .

b) Leaky Wave Region

In this region, the effective index is less than n_2 . That is $\beta/k_0 < n_2$. Leaky waves occupy the medium (j=2) which behaves as an infinite substrate.

The transverse propagation constants are defined by :

$$\delta^2_j = n^2_j\, k_0 - \beta^2 \quad j = 1, 2\ , (13a)$$

and

$$\tau_j = \beta - n_j\, k_0 \quad j = 3\ . (13b)$$

The distribution of the field is a standing wave in the film (j=1) , evanescent wave in medium (j=3) and outward propagating wave in medium (j=2) ; hence

$$Ey = A'j\ \text{Exp}\left(-x\ |\tau_j|\right)\ j = 3\ , (14a)$$

$$Ey = Aj\ \text{Exp}\left(-j\,x\ \delta_j\right) + A'j\ \text{Exp}\left(j\,x\ \delta_j\right)\ j = 1\ , (14b)$$

and

$$Ey = Aj\ \text{Exp}\left(-j\,x\ \delta_j\right)\ j = 2\ . (14c)$$

Combining Eqs. (9) , (10) , (11) , (13) and (14) , one obtains the characteristic equation in the leaky wave region as :

$$\delta_1\, T - \text{Atan}\left(\frac{|\tau_3|}{\delta_1}\right) + \text{Atan}\left(j\,\frac{\delta_2}{\delta_1}\right) = q\,\pi\ , (15)$$

where q still represents the mode number and the transverse propagation constants are given by Eq. (13) .

3. Numerical Results and Discussion

The numerical solutions of all characteristic equations (also known as the eingenvalue equation) are achieved by executing the Newton-Raphson algorithm. For simplicity, the boundary to the free-space medium (j=3) is taken as perfectly reflecting. This can be justified by the fact that n_3=1 and is largely inferior to n_1 (typical practical value in integrated optics). Such an assumption is equivalent to determining the phase of Fresnel reflection coefficient at the boundary B_{31} as $-\pi$. Consequently , in all equations , each term like Atan ($|\tau_3|$ / δ_1) must be substituted by the number + π / 2 . Also as all characteristic equations involve a branch point at $\beta/k_0 = n_2$ (singularity at critical angle θ_c), it is necesary to specify a convention that decides which branch in the computer program to choose . For this purpose we set Imag [$n_2 - \beta/k_0$]$^{1/2} > 0$, for an exp (– i ω t) time convention . As far as the tapered structure of Fig. 1 is concerned ; the eigenvalue equation , Eq. (15) , elaborated through this very simple approach agrees very closely with the eigenvalue equation found

by mean of another different and more complicated approach based on the concept of Intrinsic modal analysis [6-7] . We consider the characteristic equation, Eq. (15), governing the propagation mechanism of the Fig. 1 . It determines the allowed values of the normalized propagation constant β/k_0 and describes the modes propagating not only in the guided wave region, but also in the leaky wave region. By solving Eq. (15) for complex β, the real solutions will mathematically represent the modes in the guided wave region , whereas the complex solutions will represent the modes in the leaky wave region . Consider first the real solutions of the eigenvalue Eq. (15); their computation for the ten lowest modes is depicted by Fig. 4 . It describes the possible real normalized propagation constants β/k_0 ranging in the interval $n2< \beta/k_0 < n_1$. Notice that as the normalized thickness (k_0 T) of the structure represented in Fig. 2 increases ; all propagation constants tend to have the same value (modes degeneressences) . From Fig. 4, one can deduce that as the thickness diminishes , modes cut-off occur . So these results are very useful as long as they permit us to determine numerically the exact knowledge of the cut-off thickness corresponding to different modes to exist along the structure of Fig. 1. Such solutions in Fig. 4 represent the modes in the guided region. As the normalized thickness k_0 T of the film (j=1) narrows down, β/k_0 approaches the cut-off ($\beta/k_0 = n_2$) . By further reducing T, complex solutions of Eq. (15) need to be taken into account; when cut-off occurs (incident angle θ approaches θ_c). No real solutions of the eigenvalue equation are present . Hence, β/k_0 becomes complex with a positive imaginary part. These solutions represent the modes in a new region known as the leaky wave region.

Normalized propagation

Constant (β/k_0

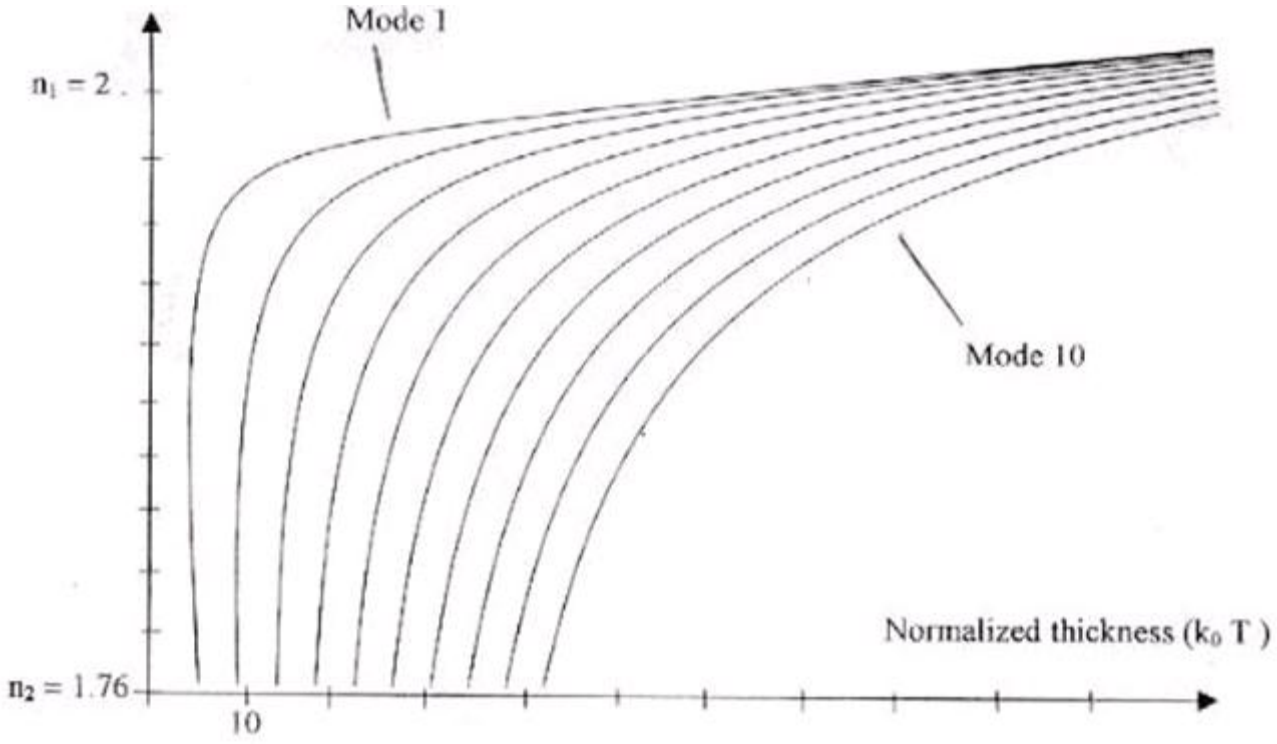

Fig. 4 : Computation of eigenvalue equation in the guided wave region for the ten lowest order modes.

Figure 5 shows systematically the behaviour of the trajectory of the leaky wave solutions for the ten lowest modes of the structure of Fig. 1 in the complex plane as T changes from a maximum normalized value (k_0 T = 100) to a minimum value (k_0 T = 0) . Any real solution in Fig. 5 represents the guided waves in the interval $n_2< \beta/k_0 < n_1$, whereas complex solutions that exist past the transition region ($\beta/k_0 = n_2$) belongs to leaky modes .

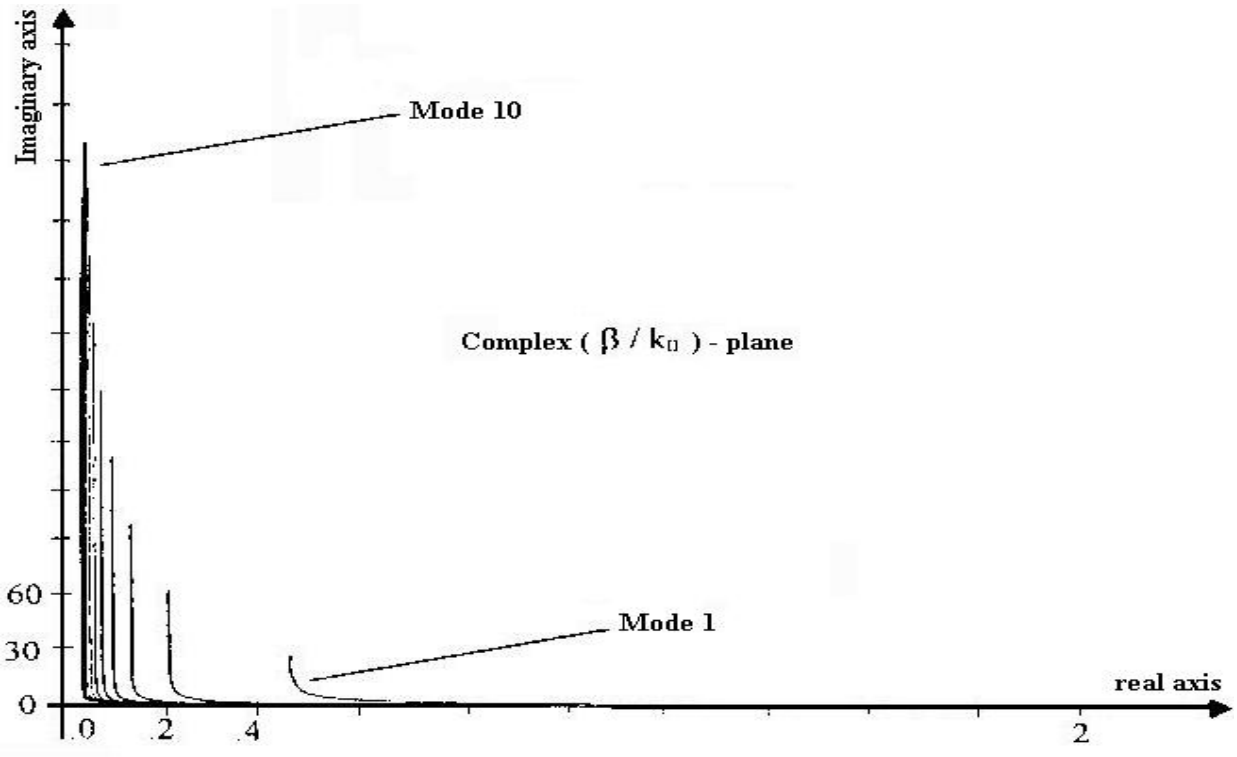

Fig. 5: Computation of eigenvalue equation in the leaky wave region for the ten lowest modes.

Solution are the complex normalized propagation constants (β/k_0) as the thickness T of the tapered waveguide diminishes (from right to left of figure).

For any modes illustrated in the complex plane of Fig. 5, it can be observed that the imaginary part of β/k_0 is positive. This is crucial to the vanishing of such leaky waves away from the transition region. Also, as the thickness T is reduced, each point on the locus sees its imaginary part getting higher in magnitude. This emphasises the fact that as the thickness T of the film (j=1) diminishes, the corresponding leaky wave launched in medium (j=2) decays more rapidly. Physically, the leaky waves describe the radiation which occurs past the transition region as the incident angle θ exceeds the critical angle θ_c of the tapered structure of Fig. 1. This physical phenomenon illustrates the coupling mechanism from medium (n_1) to medium (n_2). Figure 6 illustrates the computation of the incident angle θ defined by $\theta = A\cos(\beta/ n_1 k_0)$.

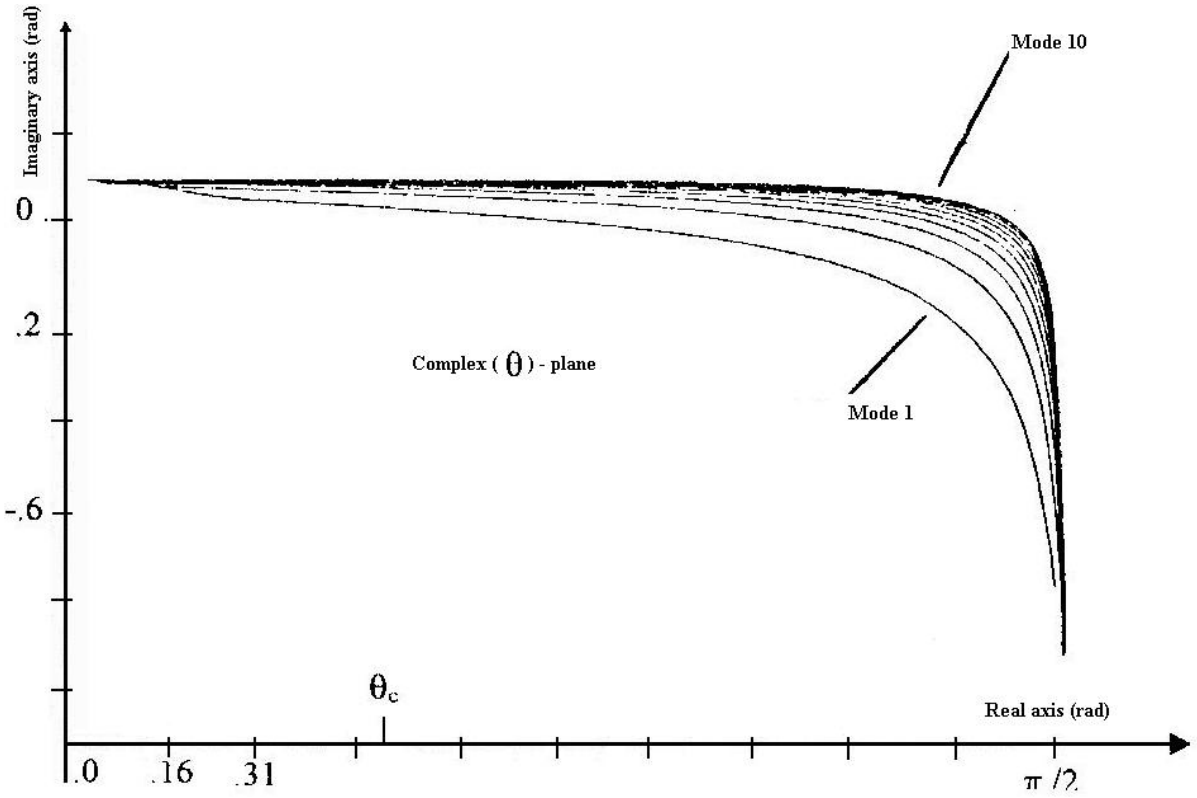

Fig. 6: Computation of eigenvalue equation in the leaky wave region for the ten lowest modes.

Solution are the complex incident angle θ (in radians) as the thickness T of the tapered waveguide is reduced (from left to right of figure).

As the thickness T varies from a maximum to a minimum value , and for the ten lowest modes of the stucture , the real solutions of θ corresponding to the guided wave region are restricted in the interval $0 < \theta < \theta_c$, whereas the complex solutions of θ coresponding to the leaky wave region are confined in the interval $\theta_c < \text{Real}\ (\theta) < \pi / 2$.

4. Conclusion

We have analyzed the tapered waveguide as illustrated by Fig. 1, using locally the conventional electromagnetic wave theory. Hereby, the tapered structure is visualized as a series of uniform steps, in which conventional wave theory for uniform guides holds. The solution of Helmoltz's equations is accomplished by suggesting in each medium as well as in each region with respect to cut-off; appropriate solutions of the field which satisfy the local boundary conditions. In this respect, we have been able to present interesting numerical results for the configuration of Fig. 1 by investigating the mode propagation in plane parallel waveguides, as the thickness T diminishes. Such a requirement is accommodated by the natural geometrical configuration of the tapered waveguide which constitutes the main body of the structure in Fig. 1. In this sense, one can unquestionably apply all numerical results concerning Fig. 2 related to structure of Fig. 1.

References:

1. A. Boudrioua , Photonic waveguide theory and applications, Lste Ltd. London, 2009.

2. M. Herlitschke , M. Blasl et F. Costache, Efficient Simulation of 3D Electro-optical Waveguides Using the Effective Refractive Index Method, Proceedings of the 2011 COMSOL Conference, October 26-28, Stuttgart, Germany, 2011.

3. I. Hunsperger, Integrated optics, theory and technology, Springe, New York , 2009.

4. V. A. Popescu , Improved Combination of Variational and Effective Index Methods for Optical Rib and Box-shaped Waveguides, Optoelectronics and Advanced Materials– Rapid Communications, Vol. 4, n. 4, pp. 459 – 464 , April 2010.

5. M.M. Ismail and M.N. Shah Zainudin , Numerical method approach in optical waveguide modeling , Applied Mechanics and Materials, Vol 52-54 , 2133-2137, 2011.

6. J. M. Arnold , A. Belghoraf and A. Dendane, Intrinsic mode theory of tapers for integrated optics; I.E.E. Proc. J. of Optoelectronics, Vol. 132,pp 34-41,1985.

7. M. Bacha and A.Belghoraf, Numerical evaluation of radiation and optical coupling occurring in optical coupler , COL 15(2), 021301(2017), Chinese Optics Letters,page 021301-1 a -5 , February 10, 2017.